

## Spin distribution measurement for $^{64}\text{Ni} + ^{100}\text{Mo}$ at near and above barrier energies

Varinderjit Singh<sup>1,a</sup>, D. Ackermann<sup>2</sup>, S. Antalic<sup>3</sup>, M. Axiotis<sup>4</sup>, D. Bazzacco<sup>5</sup>, L. Corradi<sup>6</sup>, G. De Angelis<sup>7</sup>, E. Farnea<sup>5</sup>, A. Gadea<sup>8</sup>, F.P. Heßberger<sup>2</sup>, M.G. Itkis<sup>7</sup>, G.N. Kniajeva<sup>7</sup>, E.M. Kozulin<sup>7</sup>, T. Martinez<sup>9</sup>, N. Marginean<sup>10</sup>, R. Menegazzo<sup>5</sup>, G. Montagnoli<sup>5</sup>, D.R. Napoli<sup>6</sup>, Yu. Ts. Oganessian<sup>7</sup>, M. Ruan<sup>11</sup>, R.N. Sagaidak<sup>7</sup>, F. Scarlassara<sup>5</sup>, A.M. Stefanini<sup>6</sup>, S. Szilner<sup>12</sup>, and C. Ur<sup>10</sup>

<sup>1</sup>Department of Physics, Panjab University, Chandigarh 160014, India.

<sup>2</sup>GSI Helmholtzzentrum für Schwerionenforschung GmbH, 64291 Darmstadt, Germany.

<sup>3</sup>Comenius University in Bratislava, Slovakia.

<sup>4</sup>INP Demokritos, Athens, Greece

<sup>5</sup>Dipartimento di Fisica and INFN Padova.

<sup>6</sup>INFN, Laboratori Nazionali di Legnaro, Legnaro (PD).

<sup>7</sup>JINR Flerov Laboratory of Nuclear Reaction, Dubna, Russia

<sup>8</sup>IFIC, Valencia, Spain.

<sup>9</sup>CIEMAT, Madrid, Spain

<sup>10</sup>IFIN-HH, Bucharest, Romania

<sup>11</sup>Institute of Atomic Energy, Beijing, China.

<sup>12</sup>RBI Zagreb, Croatia

**Abstract.** Spin distribution measurements were performed for the reaction  $^{64}\text{Ni} + ^{100}\text{Mo}$  at three beam energies ranging from 230 to 260 MeV. Compound nucleus (CN) spin distributions were obtained channel selective for each evaporation residue populated by the de-excitation cascade. A comparison of the spin distribution at different beam energies indicates that its slope becomes steeper and steeper with increasing beam energy. This change in slope of the spin distribution is mainly due to the onset of fission competition with particle evaporation at higher beam energies.

### 1 Introduction

Throughout the last decades, it has been well established that the nuclear structure of the collision partners, their possible deformation and coupling to inelastic channels play a vital role in the fusion process [1]. For a detailed analysis of the interaction barrier in heavy ion collisions Rowley [2] suggested a method to extract the distribution of barriers from a precisely measured fusion excitation function, enhancing structures which are due to coupling to the features mentioned above:

$$D_b = \frac{d^2 E \sigma_\ell(E)}{dE^2}.$$

These features were successfully analyzed, employing coupled channels calculations [1]. One alternative tool to study the fusion barrier is the investigation of the compound nucleus spin distribution [3] which can be written as

$$\sigma_\ell(E) = T_\ell(E, \ell)(2\ell + 1)\pi\lambda^2,$$

where the partial wave cross-section  $\sigma_\ell(E)$  is expressed as a function of the spin dependent transmission coefficient  $T_\ell(E, \ell)$  times the geometrical partial wave area, with  $\lambda$  being the de Broglie wave length. From this a transmission function of energy  $E'$  can be derived by transforming  $\ell \rightarrow E'$ :

$$E' = E - \frac{\ell(\ell + 1)}{2\mu R_b^2}$$

By subtracting for a given spin  $\ell$  the rotational barrier energy from the kinetic energy  $E$ , with  $\mu$  being the reduced mass and  $R_b$  the barrier position. The first derivative of this results in the fusion barrier distribution:

$$D_b = \frac{dT_{E'}}{dE'}.$$

<sup>a</sup>Corresponding author: Mangat\_phy@yahoo.co.in

The spin values can be obtained here by measuring  $\gamma$  multiplicities. With this method a complete barrier distribution can be measured at one beam energy. The high efficiency of  $\gamma$  multiplicity detector arrays of typically  $\approx 80\%$  helps to keep measurement times reasonably short.

Applications of this type of measurements could range from reaction mechanism studies, important for the production of exotic neutron rich species complementary to multi-nucleon transfer and preparing even for the production of super heavy nuclei in some future, to the investigation of exotic features of the neutron rich species themselves, revealing the effect those novel features like e.g. nucleon halo, neutron skin or others yet to be discovered.

One of the major goals in present day nuclear physics research is the synthesis of theoretically predicted super heavy elements (SHE). The probability that the CN may decay by fission increases with the atomic charge  $Z$  of CN. The survival probability of SHE is mainly governed by the competition between fission and particle evaporation. Hence, it becomes necessary to understand the two step process i.e. fusion/de-excitation, the entrance channel properties of the system as well as the role of the fission barrier in the exit channel. Another important aspect related to SHE production is the effect of shell closure on the survival probability of the CN, which is still not well established [4, 5]. To explore aspects like the fusion-fission competition, the role of deformation in fusion of the heavy system and a possible effect of the  $Z = 82$  shell closure on evaporation residue (ER) production, a series of experiments have been performed at the  $\gamma$  detector array GASP at the Laboratori Nazionali di Legnaro (LNL) in Legnaro(Pd), Italy, to measure the spin distribution (SD for  $^{64}\text{Ni}$ ,  $^{34}\text{S}$  and  $^{48}\text{Ca}$  induced reactions.

Here we present the results of the  $\gamma$  multiplicity measurement for  $^{64}\text{Ni} + ^{100}\text{Mo}$  reaction. The main aim of this study is to understand the effect of fission on the SD. In an earlier study for the same reaction, it was observed that the slope of the SD at high angular momentum changes with the onset of fission [6]. That measurement was carried out at the Argonne/Notre Dame BGO Array, at the Argonne National Laboratory, using an electrostatic deflector providing a global ER trigger in contrast to the here presented results were  $\gamma$  multiplicities were recorded in coincidence to individual ER channels.

## 2 Experimental Arrangements

The experiment was performed using the  $\gamma$  detector array GASP of the LNL. The array consisted of 40 Compton suppressed high purity, high efficiency germanium detectors (used here for ER identification) and a  $4\pi$  calorimeter composed of 80 BGO detectors used as  $\gamma$  multiplicity filter. The total efficiency of the multiplicity filter was  $\sim 80\%$ . The  $^{64}\text{Ni}$  beam at three energies, 230 MeV, 246 MeV and 260 MeV was bombarded on a  $^{100}\text{Mo}$  target,  $150 \mu\text{g}/\text{cm}^2$  thick evaporated on a  $15 \mu\text{g}/\text{cm}^2$  carbon backing. The energy and time spectra of each detector were recorded for offline analysis.

## 3 Data analysis and results

The energy spectra of HPGe detector were calibrated using a  $^{152}\text{Eu}$  source, and Doppler shift corrected. A two dimensional energy  $\gamma$ -fold matrix was generated. The fold (i.e. number of BGO detectors that fired) distribution was obtained for each ER channel by gating on characteristic  $\gamma$  transition energies. As example the fold distribution obtained at the lowest measured beam energy of 230 MeV is shown in Fig. 1.

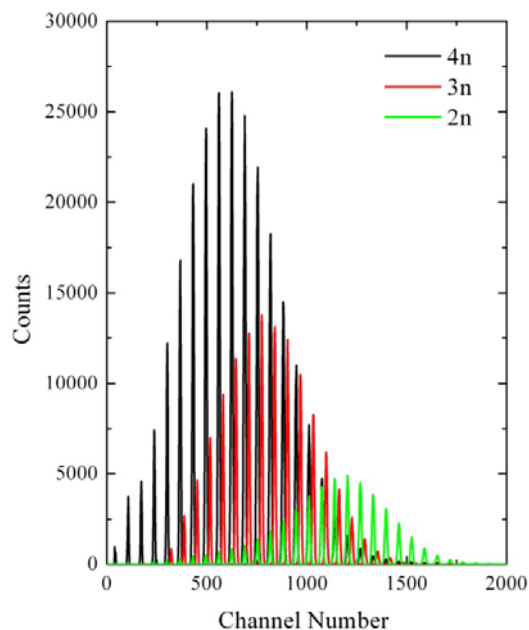


**Figure 1.** Fold distribution at the lowest beam energy of 230 MeV for the 2n, 3n and 4n evaporation channel, obtained by gating on the respective  $\gamma$ -ray transitions.

The experimentally obtained fold distribution was corrected for the relative efficiency of the HPGe detectors. The relative yield of each ER channel was obtained using the integral of the fold distribution for each ER channel, normalizing on the sum of the integral of all ER channels. This relative yield was compared with statistical model predictions, which was found to be in good agreement for 230 and 246 MeV, but deviates considerably for 260 MeV. This deviation is mainly due to the onset of fission competition with ER (see discussion below).

The obtained fold distribution was converted to a multiplicity distribution using the formalism described by Van Der Werf [7]. The response function of the GASP BGO part was obtained from the data recorded for an  $^{88}\text{Y}$  ( $\gamma$ -ray source emitting a cascade of two coincident  $\gamma$ -rays), comparing the number of detected second  $\gamma$ -rays corresponding to the measured fold for the first  $\gamma$ -ray being detected  $n$  times corresponding to the original multiplicity, with  $n$  ranging from 0 to  $n_{\text{max}}$ . The final multiplicity ( $M$ ) values were obtained employing the unfolding procedure described in the following making use of this response function which is shown in Fig. 2.

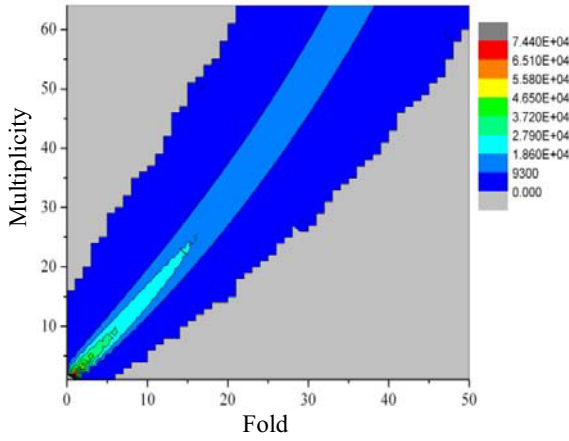


**Figure 2.** The response function of the BGO part of GASP obtained using the  $\gamma$ -ray cascade of an  $^{88}\text{Y}$  source (see text).

The multiplicity is derived in an iterative procedure (see e.g. [8]) from the fold distribution, where starting with a seed distribution and using the response matrix, at the end of each iteration step the obtained fold distribution is compared with the experimental fold distribution. A  $\chi^2$  minimization defines the end of the iteration when a predefined threshold  $\chi^2$ -value is reached. The multiplicity distribution, corresponding to the best fitted experimental fold distribution, is considered as the experimental multiplicity distribution (as shown in Fig. 3).

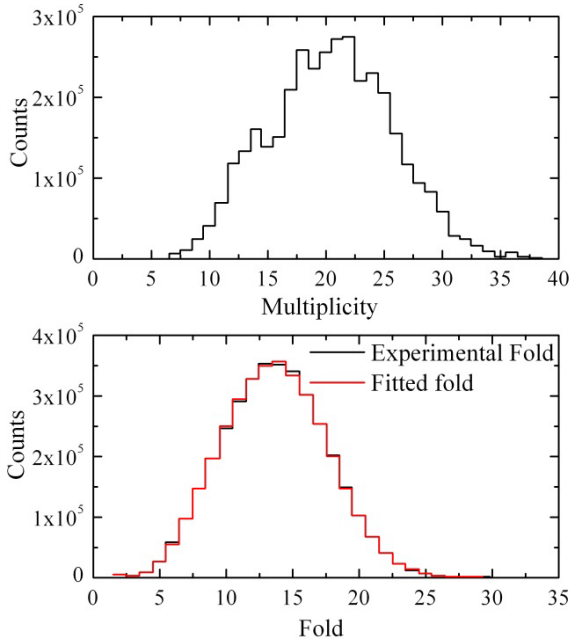


**Figure 3.** (Top) The multiplicity distribution corresponding to best fitted fold distribution. (Bottom) The comparison of experimental fold distribution with the fold distribution obtained from the multiplicity distribution after termination of the iteration.

This experimental multiplicity distribution is then converted into the SD using following expression

$$\ell_{CN} = (M_{\gamma} - M_{\gamma s})\Delta\ell_{\gamma} + M_{\gamma s}\Delta\ell_{\gamma s} + \sum M_i\Delta\ell_i + \Delta\ell_{gs/m};$$

$$i = p, n, \alpha.$$

Here  $M_{\gamma}$ ,  $\Delta\ell_{\gamma}$  and  $M_{\gamma s}$ ,  $\Delta\ell_{\gamma s}$  denote the multiplicity and spin taken away by the yrast cascade ( $\gamma$ -rays) and the statistical  $\gamma$ -rays in the early stage of the de-excitation ( $\gamma$ -rays). The sum  $\sum M_i\Delta\ell_i$  ( $i = p, n, \alpha$ ) takes into account the spin removed by the evaporated protons, neutrons and  $\alpha$ -particles, and  $\Delta\ell_{gs/m}$  is the ground state spin or of an isomeric state of the evaporation residue.

The spin removed by yrast  $\gamma$ -rays is obtained by averaging the spin removed by E1, E2 and M2 transitions for each reaction channel (given in Table 1). The multiplicity ( $M_{\ell_{\gamma s}}$ ) and spin ( $\Delta\ell_{\gamma s}$ ) of statistical  $\gamma$ -rays is taken from the statistical model code PACE2 [9]. Also the spin removed by neutrons, protons and  $\alpha$ -particles is obtained using PACE2 (given in Table 2), the corresponding evaporation particle multiplicities are obtained from the ER channels. The ground state spin of ER is taken from literature.

**Table 1.** Average spin (in units of  $\hbar$ ) removed by yrast transitions for different reaction channels.

Reaction channel	Evaporation residue	Spin removed by yrast $\gamma$ -rays( $\hbar$ )
2n	$^{162}\text{Yb}$	1.865
3n	$^{161}\text{Yb}$	1.704
4n	$^{160}\text{Yb}$	1.84
5n	$^{159}\text{Yb}$	2.00
p2n	$^{161}\text{Tm}$	1.68
p3n	$^{160}\text{Tm}$	1.2
p4n	$^{159}\text{Tm}$	1.65
$\alpha$ 2n	$^{158}\text{Er}$	1.69
$\alpha$ 3n	$^{157}\text{Er}$	1.74
$\alpha$ 4n	$^{156}\text{Er}$	1.78

**Table 2.** Average spin (in units of  $\hbar$ ) removed by the neutrons, protons,  $\alpha$ -particles and yrast  $\gamma$ -rays as function of beam energy.

Beam energy (MeV)	Neutron	Proton	$\alpha$ -particle	Statistical $\gamma$ -rays
230	0.6	0.6	2.2	0.9
246	1.2	1.2	8.1	0.9
260	1.4	1.3	8.7	1.0

The SD is obtained for each reaction channel and the summation of the SDs of all reaction channels represents the total SD of the CN as shown in Fig. 4. As expected the SDs of the ER channels are ordered from low to high spin values with decreasing number of evaporated particles, which is due to the rotational barrier reducing intrinsic excitation for increasing partial wave numbers. This behavior is terminated at a critical angular momentum  $\ell_{crit}$  where the kinetic energy for fusion is

exhausted or at higher energies as fission sets in and cuts of the spin distribution at high spin [6].

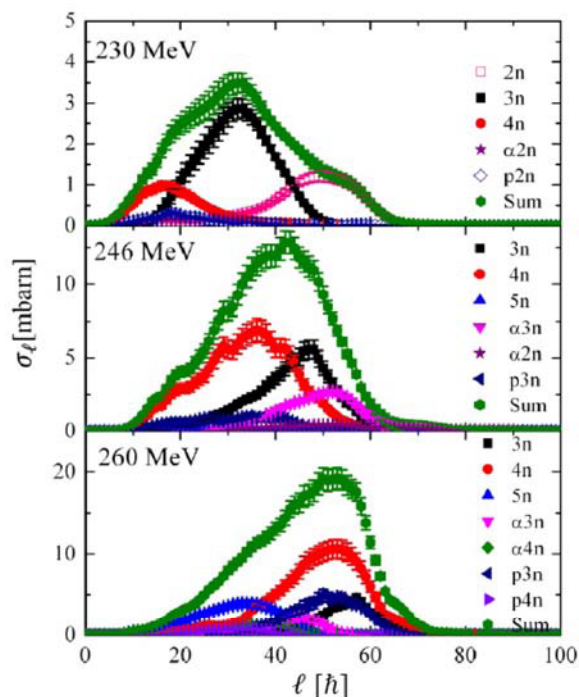


**Figure 4.** The spin distribution of different ER channels along with the sum of all channels for different beam energies is shown.

A comparison of the total SD at different energies is shown in Fig. 5. It is observed that the high spin tail of the SD becomes steeper and steeper with increasing beam energy. With increasing beam energy fission starts competing with ER production and the partial wave with higher spin end up as fission, which results in cutting of the SD at the high spin end.

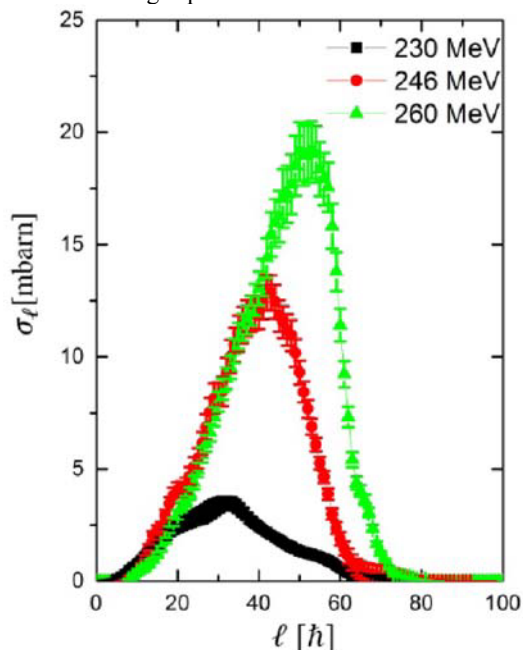


**Figure 5.** A comparison of spin distributions at different beam energies.

## 4 Conclusions

The SD has been measured for  $^{64}\text{Ni} + ^{100}\text{Mo}$  reaction. The identification of different reaction channels is performed using characteristic  $\gamma$ -ray transitions of evaporation residue. The SD is obtained for each reaction channel along with the total SD of CN. A comparison the SD at different energies shows that the fall of SD becomes more and more faster with increase in the beam energy. With increase in beam energy fission starts competing with the ER production as a results of which the partial waves with high spin end-up as fission, which results in cutting of SD at high spin end. This observation verifies the earlier observation that the onset of fission can have influence on the SD [6]. The extraction of the barrier distribution from the spin distribution is in progress.

## Acknowledgments

The financial support from the DFG as “Grant to Support Initiation of an International Collaboration” to one of the authors (V.S.) is gratefully acknowledged.

## References

1. M. Dasgupta, D.J. Hinde, N. Rowley and A.M. Stefanini, *Annu. Rev. Nucl. Part. Sci.* **48**, 401 (1998).
2. N. Rowley, G.R. Satchler and P.H. Stelson, *Phys. Lett. B* **254**, 25 (1991).
3. D. Ackermann, *Acta Physica Polonica B* **26**, 517 (1995).
4. D. Vermeulen *et al.*, *Z. Phys. A* **318**, 157 (1984).
5. Varinderjit Singh *et al.*, *Phys. Rev. C* **89**, 024609 (2014).
6. D. Ackermann *et al.*, *Nucl. Phys. A* **630**, 442c (1998).
7. S. Y. Van Der Werf, *Nucl. Instr. Meth.* **221**, 153 (1978).
8. A.H. Wuosmaa *et al.*, *Phys. Lett. B* **263**, 23(1991).
9. A. Gavron, *Phys. Rev. C* **21**, 230 (1980).